Journal of King Saud University – Computer and Information Sciences xxx (xxxx) xxx

Contents lists available at ScienceDirect

Journal of King Saud University – Computer and Information Sciences

journal homepage: www.sciencedirect.com

Entropy based automatic unsupervised brain intracranial hemorrhage segmentation using CT images

Indrajeet Kumar, Chandradeep Bhatt, Kamred Udham Singh *

Graphic Era Hill University, Dehradun, Uttarakhand, India

ARTICLE INFO

Article history:
Received 10 September 2019
Revised 1 December 2019
Accepted 5 January 2020
Available online xxxx

Keywords:
Fuzzy c-mean
Distance regularized level set evolution
Computed tomography imaging
Intracranial hemorrhage

ABSTRACT

The present work proposes entropy based automatic unsupervised brain intracranial hemorrhage segmentation using CT images. The proposed work is consisting of fuzzy c-mean (FCM), automatic selection of cluster, skull removal, thresholding and edge-based active contour methods. The FCM is used to divide the image into different cluster and among these clusters one is automatically selected for the segmentation process which have skull and hemorrhage region. Due to major benefits of level set method i.e. use large time step which reduce the number of iterations and does not need reinitialization process thus it has fast convergence speed is used for smoothness of hemorrhage region. The seed point for level set method is initialized by entropy based thresholding techniques.

The exhaustive experimentations have been carried out on 35 different patients CT images collected from SGRR Institute of Medical & Health Sciences and SMI Hospital, Dehradun, Uttarakhand, India. The performance of developed automatic segmentation techniques for hemorrhage detection is analyzed by using sensitivity, specificity, Dice coefficient, Jaccard index, Precision and Accuracy. After the evaluation of proposed method it can be observed that hemorrhagic regions segmented by the proposed method, has high accuracy comparison to FCM method and manual fuzzy based active contour method.
© 2020 The Authors. Production and hosting by Elsevier B.V. on behalf of King Saud University. This is an open access article under the CC BY-NC-ND license (http://creativecommons.org/licenses/by-nc-nd/4.0/).

1. Introduction

After the exhaustive study of literature is has been observed that intracranial hemorrhage (ICH) is major cause of death in the every region of the world of any age group (Aziz et al., 2011; Lieberman et al., 1978; Hart et al., 1984; Dalyai et al., 2011; Punitha et al., 2014; Feldmann et al., 2005; An et al., 2017; Howard et al., 2013). It occurs within the brain due to leakage of blood vessels and prevents nerve cells by communicating with the functions they control and body parts which can results in the loss of speech, memory, movement in the affected area. The major risk factors like head trauma, high blood pressure, damaged blood vessel walls, leaking of veins are directly associated with ICH (Feldmann et al., 2005; An et al., 2017; Howard et al., 2013).

There are so many imaging modalities like X-ray, MRI, CT, PET, SPECT are available for brain hemorrhage imaging, among these CT scan is widely used for detection of hemorrhage due to low cost, widely available, taking short time for imaging. So CT scan is opted as the first choice for the diagnosis of ICH (Heit et al., 2017; DeLaPaz et al., 1984; Gomez, 2008; Siddiqui et al., 2011). The appearance of the ICH clots on CT images depends on physical factors like location, density, volume, slice thickness as well as technical factor like scanning angles (Gomez, 2008; Siddiqui et al., 2011). The sample images of normal brain CT image and ICH brain CT image taken from used dataset is shown in Fig. 1.

The early detection of ICH is clinically significant for better treatment and adequate scheduling of scanning. Therefore, so many research groups are developing computer assisted CAD system for ICH segmentation. The developed computer assisted CAD system in past for segmentation of ICH is based on (a) automatic segmentation in which hemorrhage detected without any experts intervene or (b) manual segmentation in which there is need of expert for giving correct input for segmentation. It is worth to mention that so many works have been done in manual segmentation and a very few study have been done on automatic segmentation for ICH. Thus, in this work entropy based automatic unsupervised brain intracranial hemorrhage segmentation using brain CT images has been proposed.

* Corresponding author.
E-mail address: kamredudhamsingh@gmail.com (K.U. Singh).
Peer review under responsibility of King Saud University.

Production and hosting by Elsevier

https://doi.org/10.1016/j.jksuci.2020.01.003
1319-1578/© 2020 The Authors. Production and hosting by Elsevier B.V. on behalf of King Saud University.
This is an open access article under the CC BY-NC-ND license (http://creativecommons.org/licenses/by-nc-nd/4.0/).

Please cite this article as: I. Kumar, C. Bhatt and K. U. Singh, Entropy based automatic unsupervised brain intracranial hemorrhage segmentation using CT images, Journal of King Saud University – Computer and Information Sciences, https://doi.org/10.1016/j.jksuci.2020.01.003

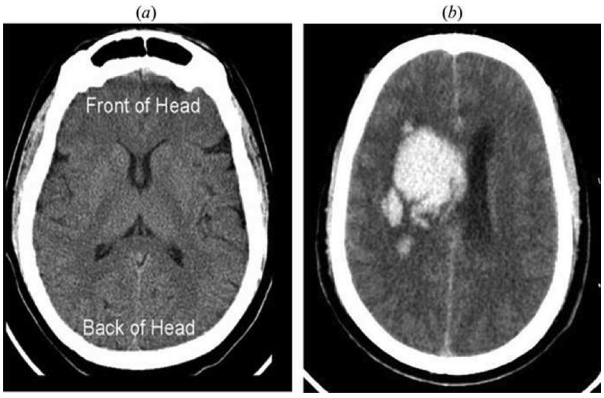

Fig. 1. Sample images taken from self collected dataset (a) normal CT scan slice of brain (b) slice of brain CT image having ICH.

The outcome of earlier studies shows that the widely used methods for ICH detection is concentrated around (a) global thresholding (Weszka et al., 1974), (b) fuzzy logics (Pham and Prince, 1999) and (c) level set active contour (Caselles et al., 1993). Otsu (1979) proposed automatic threshold selection of gray image segmentation, which classified the image pixels into two classes. Loncaric et al. (1998, 1999) has contributed for classification of objects using fuzzy c mean. Chan (2007) detects the hemorrhagic region by using left–right asymmetry and top-hat transform, which can be used to identify small hemorrhagic region. Further, Liao et al. (2010) proposed a method for automatic hematoma detection that is based on multi-resolution 0 or 1 level set approach. Zaki et al. (2011) proposed the multi-level segmentation in which multi-level fuzzy c-mean and two-level Otsu thresholding methods are used to remove abnormalities in brain CT images and then multi-level FCM is used to remove skull and background region. After that two-level Otsu method is used to segment the intracranial structure of brain hemorrhage using CT images.

Active contour model is a dynamic curve that moves within image domain and this model is used for capture actual objects boundaries. Level sets and snakes are two main mathematical models used for the active contours implementation. Snakes (Kass et al., 1988) is energy minimization spline which is controlled by external forces and explicitly moves towards the edges while level set (Osher and Sethian, 1988) method moves the active contours implicitly. Active contour model is classified into (a) edge based active contour model and (b) region based active contour model. The edge-based active contour models (Caselles et al. (1997) use an edge detector for moving the contour toward the object, which based on image gradient. Region-based active contour models use region descriptors to find the region of interest (ROI) for controlling the motion of contour. Chan and Vese (1999) proposed active contour model, which based on level set method and Mumford and Shah (1989) functional technique. In this method it's not necessary to define the boundaries of objects by gradient and initial curve can be located anywhere in the image. Li et al. (2005) proposed a new geometric active contour formulation, which moves the level set function near to sign distance function and eliminate the re-initialization process. Bhadauria and Dewal (2014) proposed the fuzzy based active contour method in which Fuzzy membership function is used to initialization of active contour. Initialized active contour moves toward the object boundaries. Fuzzy clustering is used to calculate the controlling parameter of the contour.

In literature, entropy based thresholding method was also used for segmentation of tumor (Rajinikanth et al., 2017). In this study a threshold value is decided with the help of entropy and accordingly segmentation is performed and found good results for the study of tumor segmentation. In the same manner entropy, based segmentation used for fault detection, feature selection and so on (Kapur et al., 1985; Tsallis, 1988; Rao et al., 2011; Vakharia et al., 2015; Qaroush et al., 2019). In recent research paradigm, deep learning model based segmentation is widely used. There are so many studies available based on deep learning model based segmentation (Kooi et al., 2017; Wang et al., 2016; Lévy and Jain, 2016; Dhungel et al., 2015; Bellotti et al., 2006; Chang et al., 2018; Hossain, 2019). The major limitation of such type of developed system is costly and expensive. Therefore, the present work is developing an automated ICH segmentation using entropy based thresholding techniques.

In this paper, automatic unsupervised brain intracranial hemorrhage segmentation is proposed. The proposed method has been validated on brain CT images. The concept of entropy and unsupervised are used to develop the automatic segmentation system. The proposed work comprised of fuzzy c-mean (FCM) clustering, automatic selection of cluster, skull removal, thresholding and edge-based active contour methods. The FCM is used for dividing the image into different cluster and among these clusters, one is automatically selected for the segmentation process, which have skull and hemorrhage region.

The next section i.e. Section 2 of the manuscript is providing the brief description and covering the background aspect of fuzzy c mean, entropy based thresholding and edge based active contour method. Section 3 describes the methodological framework of entropy based automatic unsupervised brain intracranial hemorrhage segmentation using brain CT images, Section 4 deals with the segmentation results and discussion and Section 5 presents the concluding remarks.

2. Methodologies

The used methodologies to develop entropy based automatic unsupervised brain intracranial hemorrhage segmentation using brain CT images are described here.

2.1. Fuzzy c-mean

Fuzzy c-mean clustering is an algorithm, which creates c-partitions of input dataset. Each partition has membership value of each data in given dataset and membership value ranges between 0 and 1. Fuzzy c-mean clustering divides the image into meaningful regions which are in the form of homogeneous. In medical image segmentation FCM (Bezdek and Pal, 1992; Bhadauria and Dewal, 2014) is widely used algorithm for fuzzy clustering.

Fuzzy c-mean clustering has been successfully applied for clustering, feature analysis and classifier design in computer assisted digital image segmentation framework or computer assisted diagnostic system (CAD). Image can be representing in different feature spaces and FCM groups the similar data type in a feature space into cluster. Membership value will be high if pixel is close to the centroid of clusters and membership value will be low if pixel is far from centroid of the clusters.

The objective function of FCM is divide $\{y_p\}_{p=1}^{N}$ into c clusters, which is defined as expression given in Eq. (1).

$$J = \sum_{i=1}^{c} \sum_{p=1}^{N} u_{ip}^{m} \| y_p - v_i \|^2 \quad (1)$$

where gray value of pth pixel is denoted by y_p ith cluster center is denoted by v_i, membership value of pth pixel is denoted by u_{ip}, fuzziness of resultant segmentation is controlled by parameter m.

Please cite this article as: I. Kumar, C. Bhatt and K. U. Singh, Entropy based automatic unsupervised brain intracranial hemorrhage segmentation using CT images, Journal of King Saud University – Computer and Information Sciences, https://doi.org/10.1016/j.jksuci.2020.01.003

The estimation of cluster center v_i and membership function u_{ip} are calculated by using Eqs. (2) and (4), respectively.

$$u_{ip} = \frac{\| y_p - v_i \|^{-2/m-1}}{\sum_{j=1}^{c} \| y_p - v_j \|^{-2/m-1}} \tag{2}$$

The used condition for defining membership function for this study is expressed in Eq. (3).

$$\sum_{i=1}^{c} u_{ip} = 1 \forall P; \quad u_{ip} \in [0,1] \tag{3}$$

$$v_i = \frac{\sum_{p=1}^{N} u_{ip}^m x_p}{\sum_{p=1}^{N} u_{ip}^m} \tag{4}$$

It is prior known that the objective function defined in Eq. (1) is an optimization problem, so the solution obtained by FCM i.e. v_i is at minimal point of defined cost function.

2.2. Edge based active contour

Edge based active contour model is widely used method to move active contour towards the boundaries of objects. So, edge data plays an significant role in moving the contour towards the object (Pratondo et al., 2017; Pratondo et al., 2017; Chen et al., 2019). It uses level set method for the motion of contour. Osher and Sethian proposed a level set evolution method (Sethian, 2001) in which level set function (LSF) represents the contour as $C = \{(i,j)/(i,j) = 0\}$ and zero LSF $\varphi(t,i,j)$ at time t gives the evolution of this contour. The LSF evolution is defined in Eq. (5).

$$\frac{\partial \phi}{\partial t} = |\nabla \phi| B, \quad \phi(0,i,j) = \phi_0(i,j) \tag{5}$$

where B represents the speed function and $\varphi_0(i,j)$ represents the initial contour.

A general level set method generates irregularities in its evolution, which leads to destroy the stability and re-initialization of level set method and affects numerical accuracy. For removing this problem Li et al. (2010) proposed, a new level set method called distance regularized level set evolution (DRLSE), in which level set method's regularity has been maintained intrinsically during level set evolution. DRLSE Level set evolution can be derived as: gradient flow, which minimizes the energy function with distance regularization term and external energy, which is used for movement of Zero level set function towards the object boundaries. DRLSE allows more efficient and flexible initialization than signed distance function. DRLSE formulations in edge based active contour model allow using large time steps, which significantly reduce the computation time and number of iteration and while maintaining numerical accuracy. The energy formulation for DRLSE is given in Eq. (6).

$$\frac{\partial \phi}{\partial t} = \mu div(d_p(|\nabla \phi|)\nabla \phi) + \lambda \delta_\varepsilon(\phi) div\left(g \frac{\nabla \phi}{|\nabla \phi|}\right) + \alpha g \delta_\varepsilon(\phi) \tag{6}$$

The first term used in Eq. (6) is known as distance regularization parameter that is also known as level set regularization parameter, μ and λ are coefficient of energy function $L_g(\varphi)$ and $A_g(\varphi)$, respectively. Further, the coefficients of energy function are regulated by expression used in Eqs. (7) and (8).

$$L_g(\phi) \underline{\underline{\Delta}} \int_\Omega g \delta(\phi) |\nabla \phi| dx \tag{7}$$

and

$$A_g(\phi) \underline{\underline{\Delta}} \int_\Omega g H(-\phi) dx \tag{8}$$

here,δ and H is known as Dirac delta function and Heaviside function. In energy functions $A_g(\varphi)$ and $L_g(\varphi)$, Heaviside function (H) and Dirac delta function (δ) are approximated by smooth function δ_ε and H_ε respectively. The parameters δ_ε and H_ε are define in Eqs. (9) and (10).

$$\delta_\varepsilon(x) = \begin{cases} \frac{1}{2\varepsilon}\left[1 + \cos\left(\frac{\pi x}{\varepsilon}\right)\right], & |x| \leqslant \varepsilon \\ 0, & |x| > \varepsilon \end{cases} \tag{9}$$

$$H_\varepsilon(x) = \begin{cases} \frac{1}{2}\left(1 + \frac{x}{\varepsilon} + \frac{1}{\pi}\sin\left(\frac{\pi x}{\varepsilon}\right)\right), & |x| \leqslant \varepsilon \\ 1, & |x| > \varepsilon \\ 0, & |x| < -\varepsilon \end{cases} \tag{10}$$

Where smooth function δ_ε is the derivative of smooth function H_ε. In the formulation of DRLSE, binary step function is initialized as define in Eq. (11).

$$\phi_0(x) = \begin{cases} -c_0, & x \in R_0 \\ c_0, & otherwise \end{cases} \tag{11}$$

where c_0 is a constant parameter and R_0 is the region in domain Ω.

2.3. Entropy based thresholding

Thresholding is a technique used to segment the image into background and foreground region. In this work entropy based thresholding which computes a threshold value based on the information content of the histogram on input image (Kumar et al., 2014; Malik et al., 2016; Liscano and Wong, 1995; Rawat et al., 2014; Zhang and Liu, 2006). In this process Shannon's information entropy has been computed by maximize the amount of information between two parts of the histogram with respect to the threshold point in the histogram.

Let's assume that two sections A as foreground and B as background for an input image have the probability distributions as

$$A : \frac{p_1}{p_s}, \frac{p_2}{p_s}, \frac{p_3}{p_s}, ..., \frac{p_s}{p_s} \tag{12}$$

$$B = \frac{p_s+1}{1-p_s}, \frac{p_s+2}{1-p_s}, \frac{p_s+3}{1-p_s}, ..., \frac{p_n}{1-p_s} \tag{13}$$

where $p_i : i = 1, 2, ..., n$is the probability associated with the location in the histogram and $p_s = \sum_{i=1}^{n} p_i$, The value associated with location s in the histogram is considered as the threshold value.

Now the entropy associated to these points are computed by applying Shannon's entropy information equation as

$$H(A) = -\sum_{i=1}^{s} \frac{p_i}{p_s} \ln \frac{p_i}{p_s} = \ln p_s + \frac{H_s}{p_s} \tag{14}$$

And

$$H(B) = -\sum_{i=s+1}^{n} \frac{p_i}{1-p_s} \ln \frac{p_i}{1-p_s} = \ln(1-p_s) + \frac{H_n - H_s}{1-p_s} \tag{15}$$

where $H_n = -\sum_{i=1}^{n} p_i \ln p_i$ is known as entropy over whole histogram, and $H_s = -\sum_{i=1}^{s} p_i \ln p_i$ is entropy for the location under the threshold location s.

The overall entropy for this work for input image is defined as the sum of H(A) and H(B). Hence the expression would be written as

Please cite this article as: I. Kumar, C. Bhatt and K. U. Singh, Entropy based automatic unsupervised brain intracranial hemorrhage segmentation using CT images, Journal of King Saud University – Computer and Information Sciences, https://doi.org/10.1016/j.jksuci.2020.01.003

$$H = H(A) + A(B) = \ln p_s(1-p_s) + \frac{H_s}{p_s} + \frac{H_n - H_s}{1-p_s} \quad (16)$$

The threshold value is defined as the location in the histogram where the maximum value of H.

3. Proposed method

In this work, entropy based automatic unsupervised brain intracranial hemorrhage segmentation using brain CT images has been proposed. The proposed work comprised of fuzzy c-mean (FCM) clustering, automatic selection of cluster, skull removal, thresholding and edge-based active contour methods. The FCM is used for dividing the image into different cluster and among these clusters, one is automatically selected for the segmentation process, which have skull and hemorrhage region.

The methodological framework for entropy based automatic unsupervised brain intracranial hemorrhage segmentation using fuzzy c-mean with edge-based active contour on brain CT images is shown in Fig. 2.

Initially FCM is applied on the brain CT images in which a clustered image is automatically selected, then skull is removed from the selected clustered image and threshold it by entropy based thresholding method. After thresholding resultant clustered image is used to initialize the DRLSE method.

3.1. Fuzzy c mean

Fuzzy c mean segmentation is used to divide image into different clusters and these clusters have similar type of membership values. In proposed work FCM divides all hemorrhagic images into three different clusters. FCM divides the hemorrhagic images into only three clusters because one of them gives the skull with hemorrhagic region. So in the proposed work we have fixed the value of c = 3 in Eqs. (1) and (2).

3.2. Automatic selection of cluster

A cluster is automatically selected among three clusters by matching the skull histogram of CT image with the FCM clustered images. A FCM clustered image Y(i, j) which have highest match with CT skull histogram is selected for further processing.

3.3. Skull removal

The skull is removed from the selected $Y(i,j)$ image by multiply an image $P(i,j)$ with the $Y(i,j)$ image. Image $P(i,j)$ is given as

$$P(i,j) = \begin{cases} 1 & inside \quad A \\ 0 & outside \quad A \end{cases} \quad (17)$$

$$X(i,j) = Y(i,j) * P(i,j) \quad (18)$$

where A is the skull region of original CT image which is obtained by thresholding highest intensity pixels of the original CT image at t threshold, and X is the image which has hemorrhagic region with removed skull. Threshold t can be fixed for all hemorrhagic images.

3.4. Entropy based thresholding

Entropy based thresholding is used to segment the image. It also removes ventricles of image X. the obtained threshold values from Eq. (16) is used for hemorrhagic images to process the input images for detection of hemorrhagic region. The resultant image for input image X gives the hemorrhagic region and some spurious blobs. Spurious blobs are removed by the morphological operations: erosion and dilation. Erosion used to shrink the objects which remove the spurious blobs and dilation is used to recover or expand the objects. Let $Z(i,j)$ is the resultant image after thresholding and morphological operation.

3.5. Fuzzy segmented image with DRLSE

After thresholding and morphological operations, resultant hemorrhagic image $Z(i,j)$ is used to initialize the DRLSE method. DRLSE use binary step function to initialize the level set method. The defined binary step function $\varphi_0(x,y)$ in Eq. (6) uses the image $Z(i,j)$ for getting the value of hemorrhagic region.

Initial contour $\varphi_0(x)$ placed inside the hemorrhagic region so the value of α is set to negative. The term g used in Eq. (6) takes smaller values at boundaries and when active contour arrive at objects boundaries then it slow down the expanding of zero level contour. Term g can be calculated as

$$g = \frac{1}{1 + |\nabla G_r * I|^2} \quad (19)$$

where G_r denotes Gaussian kernel having standard deviation (r) and I denotes original image. The initialization of level set method is performed using Eq. (20).

$$\phi_0(x,y) = z(i,j) \quad (20)$$

There are so many controlling parameters in level set method that are given manually for different hemorrhagic images. But in DRLSE method controlling parameter can be fixed for hemorrhagic images as time step (Δt) set to 1.0, λ set to 5.0 and μ can be calculated as

$$\mu = \frac{0.2}{\Delta t} \quad (21)$$

The edge based active contour method uses DRLSE which has large time step, minimize the number of iterations and maintain numerical accuracy. Segmentation of proposed method and existing methods are shown in following Fig. 3.

3.6. Performance evaluation parameters

In this work the performance of proposed hemorrhage segmentation technique is analyzed by the parameters like sensitivity, specificity, Dice coefficient, Jaccard index, Precision and Accuracy. The original depict hemorrhage on ICH is manually drawn by the radiologist (also co-author of this manuscript) is used as ground truth segmented region. The value of these ground truth hemorrhage are compared with the value of proposed segmentation result. The performance parameters are calculated using

$$Sensitivity \quad \% = \left(\frac{TP}{FN+TP}\right) * 100 \quad (22)$$

$$Specificity\% = \left(\frac{TN}{FP+TN}\right) * 100 \quad (23)$$

$$Precision\% = \left(\frac{TP}{TP+FP}\right) * 100 \quad (24)$$

$$Accuracy\% = \left(\frac{TP+TN}{TP+FP+TN+FN}\right) \quad (25)$$

Where, True positive (TP) is a pixel which is present in both ground truth hemorrhage and proposed segmented hemorrhage. True negative (TN) is a pixel which is absent in both ground truth hemorrhage and proposed segmented hemorrhage. False positive (FP) is a pixel which is present in the ground truth hemorrhage

Please cite this article as: I. Kumar, C. Bhatt and K. U. Singh, Entropy based automatic unsupervised brain intracranial hemorrhage segmentation using CT images, Journal of King Saud University – Computer and Information Sciences, https://doi.org/10.1016/j.jksuci.2020.01.003

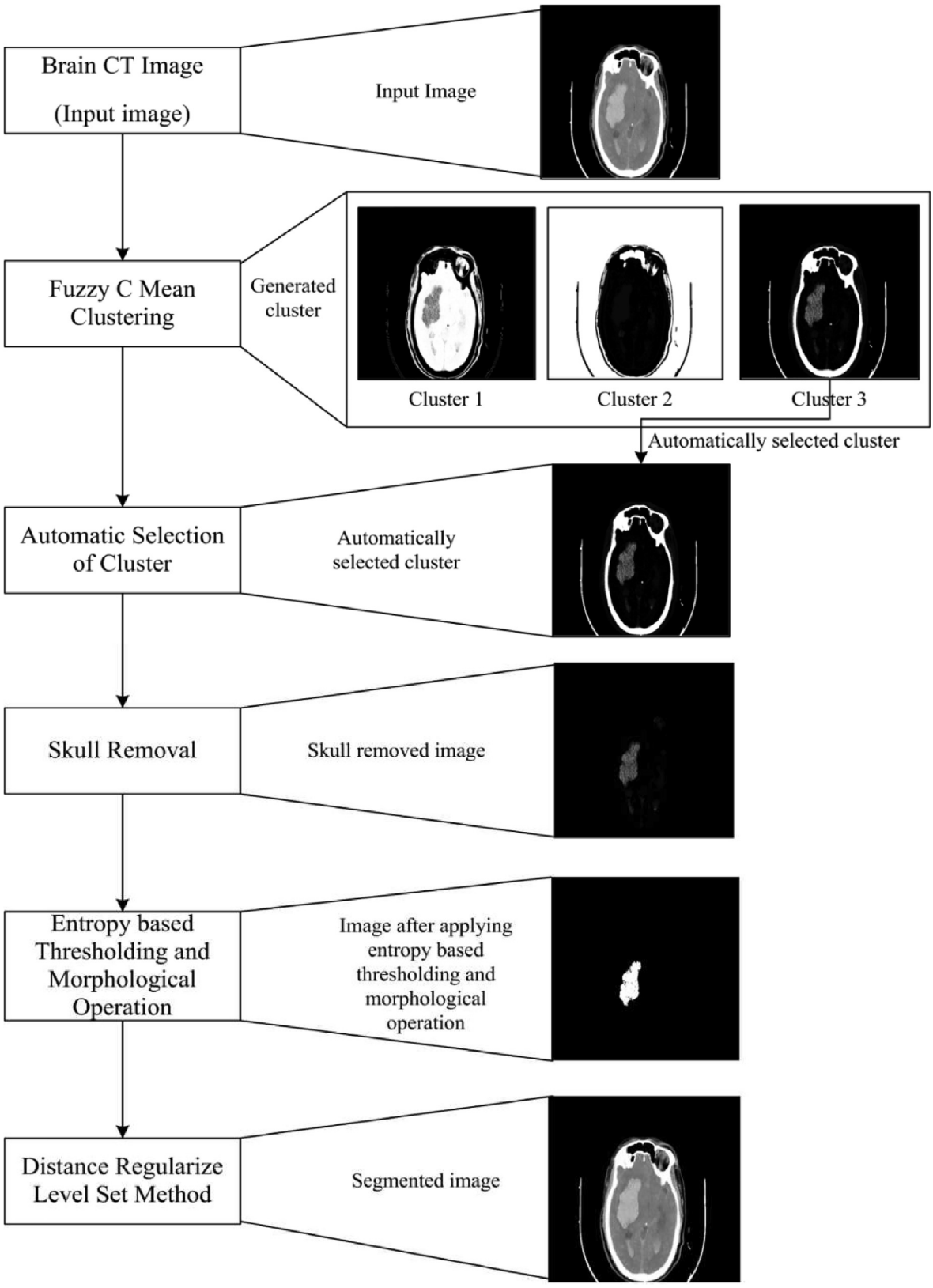

Fig. 2. Proposed methodology flowchart.

border but absent in proposed segmented hemorrhage. False negative (FN) is a pixel which is absent in ground truth hemorrhage border but present in proposed segmented hemorrhage.

Jaccard index is defined as an estimation of similarity between two or more sample sets. Jaccard index and Dice coefficient can be computed as

Please cite this article as: I. Kumar, C. Bhatt and K. U. Singh, Entropy based automatic unsupervised brain intracranial hemorrhage segmentation using CT images, Journal of King Saud University – Computer and Information Sciences, https://doi.org/10.1016/j.jksuci.2020.01.003

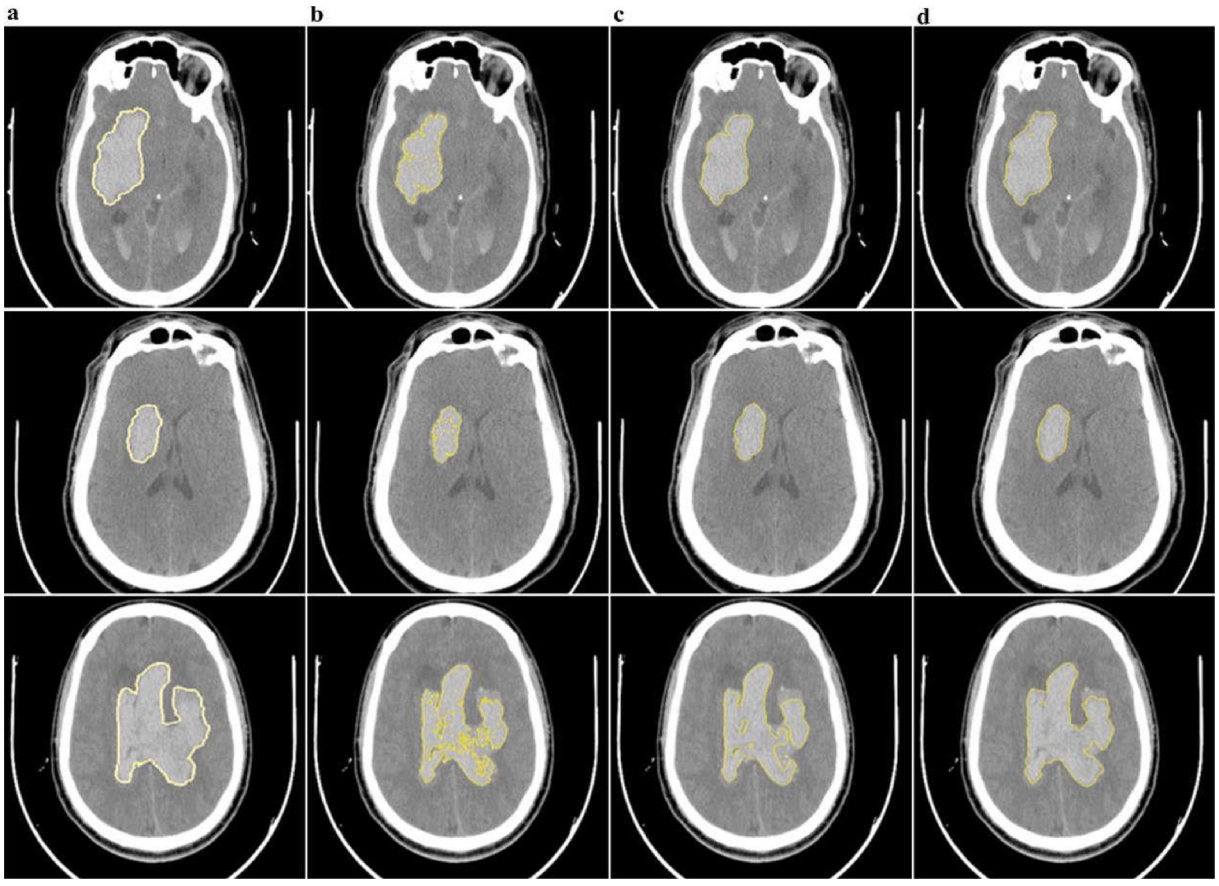

Fig. 3. Hemorrhage segmentation of CT image: column (a) original image (b) FCM clustering method (c) Manual fuzzy based active contour method (d) Proposed method.

$$Jaccard \quad index = \frac{R_{MS} \cap R_{PS}}{R_{MS} \cup R_{PS}} \tag{26}$$

$$Dice \quad coefficient = 2 * \frac{R_{MS} \cap R_{PS}}{R_{MS} + R_{PS}} \tag{27}$$

where R_{PS} represents the hemorrhagic region segmented by proposed work and R_{MS} represents the hemorrhagic region of manual segmentation.

4. Experimental results and analysis

4.1. Dataset description

The proposed segmentation method for ICH is validated on a dataset of 35 patients suffering from ICH. A total of 35 brain ICH CT images are collected from the Shri Guru Ram Rai Institute of Medical & Health Science, Dehradun and Shri Mahant Indresh Hospital, Dehradun, Uttarakhand, India during March 2016 to August 2017. The age group of considered patients is between twenty seven to sixty nine. The Philips Mx16 is used as a scanning device for capturing brain CT images. The size of captured brain CT images is of 512 × 512 pixels having the thickness of 2.5 mm. The image dataset consisting of 35 cases are stored in a workstation (HP Z420D) having configuration of processor Intel®Xeon® 3.00 GHz and 8 GB of RAM. All simulation tasks has been performed on same system in Matlab-2017 environment. The brief description of dataset is given in Table 1.

Table 1
Description of dataset.

Image Source	Shri Guru Ram Rai Institute of Medical & Health Science, Dehradun and Shri Mahant Indresh Hospital, Dehradun, Uttarakhand, India
Total Number of images	35 (20 + 15)
Scanner type	Philips Mx16
Image resolution	512 × 512 pixels
Thickness	2.5 mm.

4.2. Experimental results

It is worth to mention that the proposed segmentation method is different from the fuzzy based active contour. It requires an expert person involvement for manually giving the best cluster for initialization of level set method while in case of proposed method there is no need of any expert person involvement to initialize the level set method. The proposed method automatically select the appropriate cluster for level set method initialization and segment the desired region of ICH from any input brain CT scan images. The sample images of ICH segmentation using fuzzy based active contour segmentation, fuzzy clustering based segmentation and proposed segmentation method is shown in Fig. 4.

It has been observed from the Fig. 4 that the accuracy of extracted hemorrhagic region of proposed method is highest than fuzzy clustering segmentation and fuzzy based active contour segmentation.

The Proposed segmentation technique is applied on each cases of dataset having various types and shapes of ICH. The obtained results are reported in Table 2 and the Results of proposed method

Please cite this article as: I. Kumar, C. Bhatt and K. U. Singh, Entropy based automatic unsupervised brain intracranial hemorrhage segmentation using CT images, Journal of King Saud University – Computer and Information Sciences, https://doi.org/10.1016/j.jksuci.2020.01.003

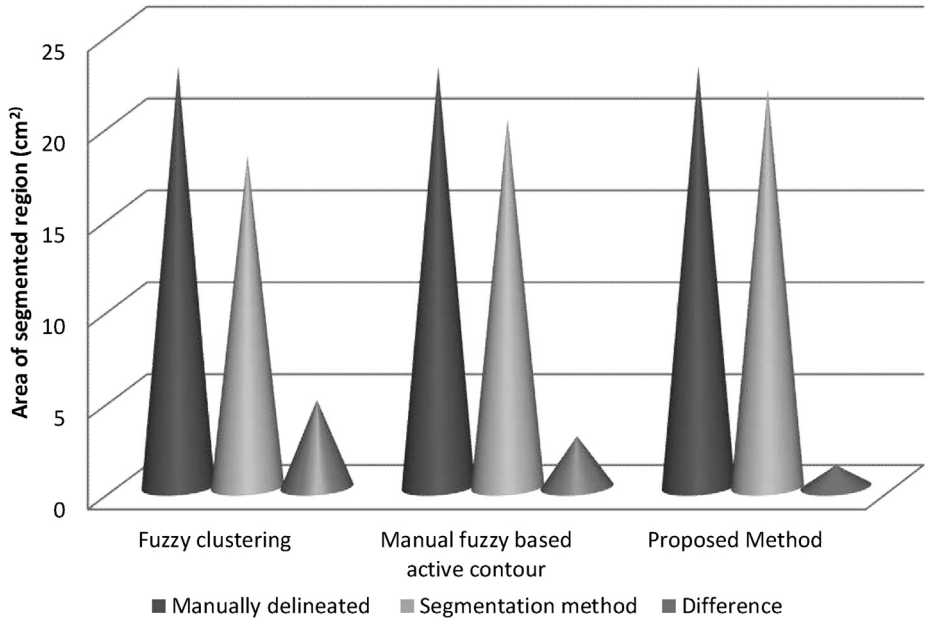

Fig. 4. Comparative analysis of results in terms of segmented area by using fuzzy clustering method, manual fuzzy based active contour method and proposed method.

Table 2
Comparative analysis of results in terms of segmented area by different methods.

CT image NO.	Hemorrhagic area (cm^2)						
	Manually delineated (A)	Fuzzy clustering (B)	Difference (A-B)	Manual fuzzy based active contour (C)	Difference (A-C)	Proposed work (D)	Difference (A–D)
1	18.08	13.28	4.8	17.44	0.64	17.95	0.13
2	51.10	42.34	8.76	45.39	5.71	50.53	0.57
3	60.93	51.10	9.83	53.99	6.94	58.15	2.78
4	20.41	16.69	3.72	18.54	1.87	20.37	0.04
5	23.38	18.95	4.43	19.82	3.56	22.65	0.73
6	23.44	18.58	4.86	22.53	0.91	22.53	0.91
7	6.52	4.93	1.59	5.89	0.63	6.48	0.04
8	10.69	8.33	2.36	10.61	0.08	10.63	0.06
9	16.04	12.61	3.43	15.49	0.55	15.51	0.53
10	13.76	11.19	2.57	12.48	1.28	12.55	1.21
–	–	–	–	–	–	–	–
–	–	–	–	–	–	–	–
–	–	–	–	–	–	–	–
–	–	–	–	–	–	–	–
27	8.17	5.66	2.51	7.38	0.79	7.59	0.58
28	10.07	8.00	2.07	9.45	0.62	8.84	1.23
29	12.13	8.45	3.68	10.53	1.6	10.66	1.47
30	109.27	88.15	21.12	89.24	20.03	103.58	5.69
31	5.49	4.23	1.26	5.00	0.49	5.39	0.1
32	12.06	5.89	6.17	7.48	4.58	7.57	4.49
33	29.69	25.51	4.18	27.55	2.14	28.36	1.33
34	8.89	6.28	2.61	8.01	0.88	8.27	0.62
35	11.08	7.01	4.07	8.75	2.33	9.95	1.13
Average	**22.97**	**18.14**	**4.82**	**20.15**	**2.82**	**21.76**	**1.21**

are compared with fuzzy based active contour segmentation and fuzzy clustering based segmentation using Hemorrhagic area (cm^2). The results reported in Table 2 shows the difference between expert delineated hemorrhage and different methods segmented hemorrhage.

During the tedious experimentations of fuzzy clustering method, manual fuzzy based active contour method and proposed method each case of collected dataset are segmented. The obtained segmented areas are in the range of 5.39 cm^2 to 103.58 cm^2 and average is 21.76 cm^2 for proposed work. Similarly, the segmented area for fuzzy clustering is in the range of 4.23 cm^2 to 88.15 cm^2 and 5.00 cm^2 to 89.24 cm^2 manual fuzzy based active contour method. The average difference of brain hemorrhagic area segmented by fuzzy clustering, fuzzy based active contour and proposed methods with respect to manual delineation labeled by expert radiologists are 4.82 cm^2, 2.82 cm^2 and 1.21 cm^2 respectively, which shows that the proposed method accurately segment the hemorrhagic area with highest accuracy.

After the analysis of results given in Table 2, it has been observed that the proposed method yields the better result with respect to fuzzy clustering method and manual fuzzy based active contour method.

In literature survey, it is found that the performance of segmentation method is also defined by the sensitivity, specificity, Jaccard

Please cite this article as: I. Kumar, C. Bhatt and K. U. Singh, Entropy based automatic unsupervised brain intracranial hemorrhage segmentation using CT images, Journal of King Saud University – Computer and Information Sciences, https://doi.org/10.1016/j.jksuci.2020.01.003

index and Dice coefficient. Thus, the obtained sensitivity and specificity for each CT scan image of ICH segmentation is reported in Table 3 for fuzzy clustering method, manual fuzzy based active contour method and proposed method.

From the Table 3 it has been observed that the obtained sensitivity for proposed method is varying in the range of 60.45% to 94.36% with average value of 87.06% and the obtained specificity for proposed method is varying in the range of 99.95% to 100% with average value 99.98%. Further, it has been also observed that the values of sensitivity are varying in the range of 43.03% to 82.15% for fuzzy clustering method and 62.10% to 92.60% for manual fuzzy based active contour with average value of 68.07% and 84.55% respectively. Similarly, the values of specificity are varying from 99.96% to 100% for fuzzy clustering method and 99.94% to 100% for manual fuzzy based active contour having average of 99.98 and 99.97 respectively.

The comparative analysis of obtained results in terms of sensitivity and specificity for fuzzy clustering method, manual fuzzy based active contour method and proposed method is shown in Fig. 5.

After the comparative analysis of results in terms of sensitivity and specificity among fuzzy clustering method, manual fuzzy based active contour method and proposed method found that the maximum sensitivity is achieved by the proposed segmentation method. The obtained average value of sensitivity is 68.07% for fuzzy clustering method, 84.55% is for manual fuzzy based

Table 3
Analysis of sensitivity and specificity of different segmentation methods.

CT image NO.	Sensitivity (%)			Specificity (%)		
	Fuzzy clustering	Manual fuzzy based active contour	Proposed method	Fuzzy clustering	Manual fuzzy based active contour	Proposed method
1	70.46	90.15	90.95	100	99.96	99.99
2	79.20	88.14	94.36	100	99.98	99.96
3	82.15	89.85	93.28	99.99	99.98	99.98
4	69.67	84.37	91.21	99.99	99.94	99.97
5	66.69	78.70	88.81	99.99	99.98	99.98
6	73.70	92.45	90.03	100	99.99	99.99
7	60.23	82.84	82.06	99.99	99.98	99.97
8	64.77	83.50	82.01	99.98	99.98	100
9	75.96	92.60	90.48	99.99	99.97	99.98
10	72.61	88.33	88.26	99.99	99.98	99.98
–	–	–	–	–	–	–
–	–	–	–	–	–	–
–	–	–	–	–	–	–
–	–	–	–	–	–	–
27	70.55	89.80	92.71	99.99	99.99	99.98
28	71.02	83.25	86.81	99.99	99.96	99.97
29	67.90	85.15	86.27	99.98	99.98	99.98
30	68.97	75.35	88.73	99.96	99.94	99.95
31	67.20	90.46	92.09	99.99	99.99	99.98
32	43.03	62.10	60.45	100	100	100
33	77.60	89.78	89.72	99.99	99.98	99.97
34	65.29	85.69	86.44	100	99.99	100
35	49.35	71.48	77.46	100	99.99	99.99
Average	**68.07**	**84.55**	**87.06**	**99.98**	**99.97**	**99.98**

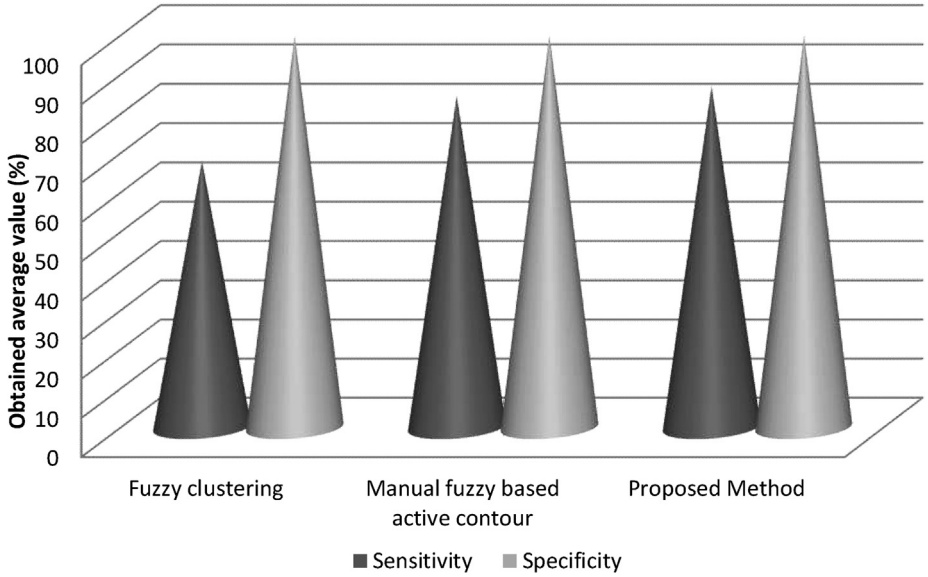

Fig. 5. Comparative analysis of results in terms of sensitivity and specificity for fuzzy clustering method, manual fuzzy based active contour method and proposed method.

Please cite this article as: I. Kumar, C. Bhatt and K. U. Singh, Entropy based automatic unsupervised brain intracranial hemorrhage segmentation using CT images, Journal of King Saud University – Computer and Information Sciences, https://doi.org/10.1016/j.jksuci.2020.01.003

active contour method and 87.06% is for proposed method. The obtained average value of specificity is 99.98% for fuzzy clustering method, 99.97% is for manual fuzzy based active contour method and 99.98% is for proposed method. The obtained value for sensitivity and specificity shows that the proposed segmentation method provides better performance and segmented the ICH region more accurately.

Further, the performance evaluation parameters Precision and Accuracy are computed for fuzzy clustering method, manual fuzzy based active contour method and proposed method using same dataset. The obtained results are given in Table 4.

From the Table 4 it has been observed that the obtained Precision for proposed method is varying in the range of 0.9696 to 1.000 with average value of 0.99207 and the obtained Accuracy value for proposed method is varying in the range of 0.9979 to 0.9997 with average value 0.9987. Further, it has been also observed that the values of Precision are varying in the range of 0.8522 to 0.9971 for fuzzy clustering method and 0.8966 to 0.9954 for manual fuzzy based active contour with average value of 0.9625 and 0.9720 respectively. Similarly, the values of Accuracy are varying from 0.9956 to 0.9993 for fuzzy clustering method and 0.9884 to 0.9997 for manual fuzzy based active contour having average of 0.9973 and 0.9983 respectively.

The comparative analysis of obtained results in terms of Precision and Accuracy for fuzzy clustering method, manual fuzzy based active contour method and proposed method is shown in Fig. 6.

After the analysis of obtained value of Precision and Accuracy for fuzzy clustering method, manual fuzzy based active contour

Table 4
Analysis of Precision and Accuracy of different segmentation methods.

CT image NO.	Precision (%)			Accuracy (%)		
	Fuzzy clustering	Manual fuzzy based active contour	Proposed method	Fuzzy clustering	Manual fuzzy based active contour	Proposed method
1	99.71	99.17	100	9.75	99.83	99.83
2	98.19	98.26	99.47	99.73	99.86	99.86
3	98.58	98.57	100	99.89	99.95	99.96
4	96.88	98.08	100	99.81	99.89	99.90
5	94.40	94.22	100	99.80	99.90	99.90
6	98.43	99.36	100	99.56	99.74	99.85
7	98.26	99.54	99.94	99.56	99.74	99.79
8	93.44	95.65	98.22	99.75	99.85	99.88
9	97.86	98.76	99.63	99.69	99.79	99.88
10	99.30	99.27	100	99.76	99.93	99.90
–	–	–	–	–	–	–
–	–	–	–	–	–	–
–	–	–	–	–	–	–
–	–	–	–	–	–	–
27	85.22	89.66	94.21	99.91	99.95	99.95
28	97.45	96.55	99.43	99.85	99.92	99.92
29	96.77	96.00	98.99	99.85	99.93	99.93
30	97.75	97.35	99.90	99.86	99.93	99.93
31	96.35	97.94	100	99.91	99.96	99.96
32	94.71	96.19	99.54	99.93	99.97	99.97
33	91.37	93.59	96.92	99.90	99.93	99.94
34	95.58	96.84	99.73	99.87	99.93	99.94
35	98.60	98.43	98.96	98.58	98.84	99.36
Average	**96.2553**	**97.0226**	**99.2074**	**997.347**	**99.8337**	**99.8763**

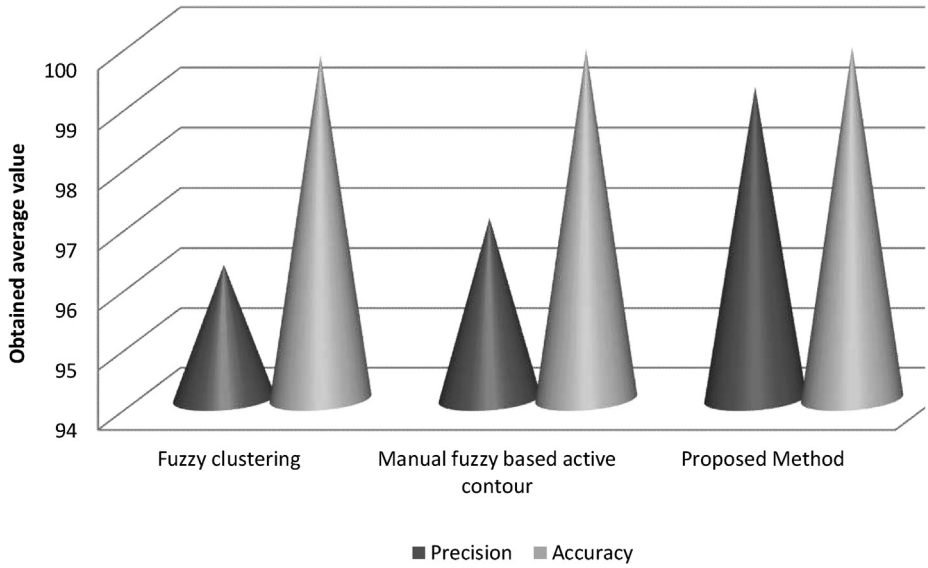

Fig. 6. Comparative analysis of results in terms of Precision and Accuracy for fuzzy clustering method, manual fuzzy based active contour method and proposed method.

Please cite this article as: I. Kumar, C. Bhatt and K. U. Singh, Entropy based automatic unsupervised brain intracranial hemorrhage segmentation using CT images, Journal of King Saud University – Computer and Information Sciences, https://doi.org/10.1016/j.jksuci.2020.01.003

method and proposed method, it has been observed that the proposed method yields better performance. The difference in obtained average Precision value is 0.02952 between proposed method and fuzzy clustering. Similarly, 0.02184 is difference between manual fuzzy based active contour method and proposed method in terms of Precision. It is worth to mention that the obtained accuracy for each method shows almost equally good but proposed method once again yields highest accuracy. Thus it has been ultimately said that the proposed segmentation method provides better performance and segment the ICH region more accurately.

Further, the performance evaluation parameters Jaccard index and Dice coefficient are computed for fuzzy clustering method, manual fuzzy based active contour method and proposed method using same dataset. The obtained results are given in Table 5.

From the Table 5 it has been observed that the obtained Jaccard index for proposed method is varying in the range of 0.67–0.94 with average value of 0.84 and the obtained Dice coefficient for proposed method is varying in the range of 0.83–0.97 with average value 0.93. Further, it has been also observed that the values of Jaccard index are varying in the range of 0.48–0.85 for fuzzy clustering method and 0.68–0.93 for manual fuzzy based active contour

Table 5
Analysis of Jaccard index and Dice coefficients of different segmentation methods.

CT image NO.	Jaccard index			Dice coefficients		
	Fuzzy clustering	Manual fuzzy based active contour	Proposed method	Fuzzy clustering	Manual fuzzy based active contour	Proposed method
1	0.75	0.88	0.88	0.86	0.94	0.93
2	0.81	0.88	0.94	0.90	0.94	0.97
3	0.85	0.91	0.93	0.92	0.95	0.96
4	0.70	0.84	0.88	0.83	0.92	0.94
5	0.69	0.80	0.89	0.82	0.89	0.95
6	0.79	0.93	0.92	0.89	0.96	0.96
7	0.62	0.79	0.77	0.80	0.90	0.89
8	0.67	0.83	0.81	0.82	0.91	0.90
9	0.79	0.90	0.89	0.89	0.95	0.94
10	0.76	0.88	0.88	0.86	0.93	0.93
–	–	–	–	–	–	–
–	–	–	–	–	–	–
–	–	–	–	–	–	–
–	–	–	–	–	–	–
27	0.74	0.89	0.90	0.86	0.94	0.95
28	0.74	0.83	0.84	0.87	0.91	0.92
29	0.72	0.87	0.87	0.85	0.93	0.93
30	0.69	0.75	0.87	0.83	0.87	0.93
31	0.71	0.89	0.88	0.84	0.94	0.94
32	0.48	0.68	0.67	0.68	0.83	0.83
33	0.80	0.90	0.89	0.90	0.95	0.94
34	0.70	0.86	0.88	0.83	0.92	0.94
35	0.53	0.77	0.82	0.72	0.89	0.92
Average	**0.71**	**0.84**	**0.86**	**0.83**	**0.91**	**0.93**

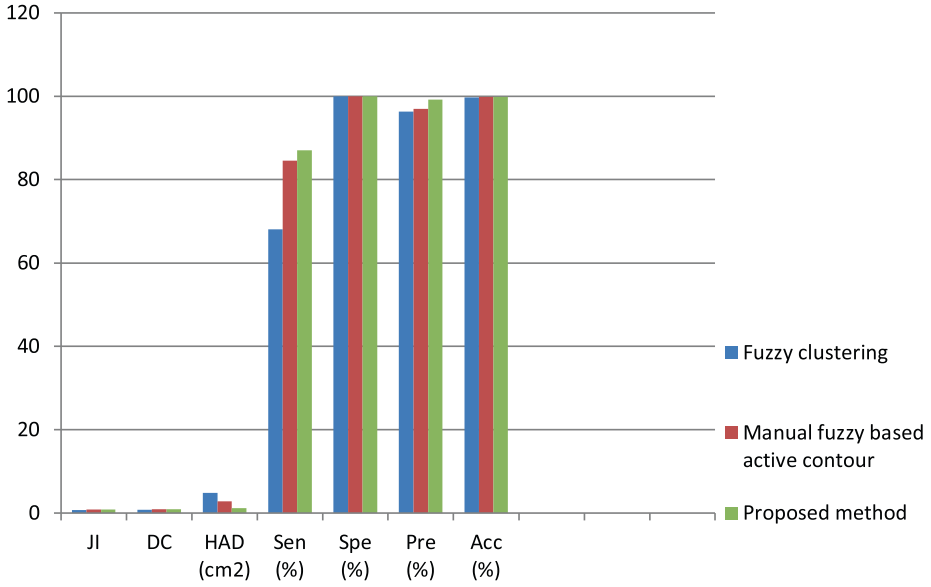

Fig. 7. Comparative analysis of results in terms of Jaccard index and Dice coefficient for fuzzy clustering method, manual fuzzy based active contour method and proposed method.

Please cite this article as: I. Kumar, C. Bhatt and K. U. Singh, Entropy based automatic unsupervised brain intracranial hemorrhage segmentation using CT images, Journal of King Saud University – Computer and Information Sciences, https://doi.org/10.1016/j.jksuci.2020.01.003

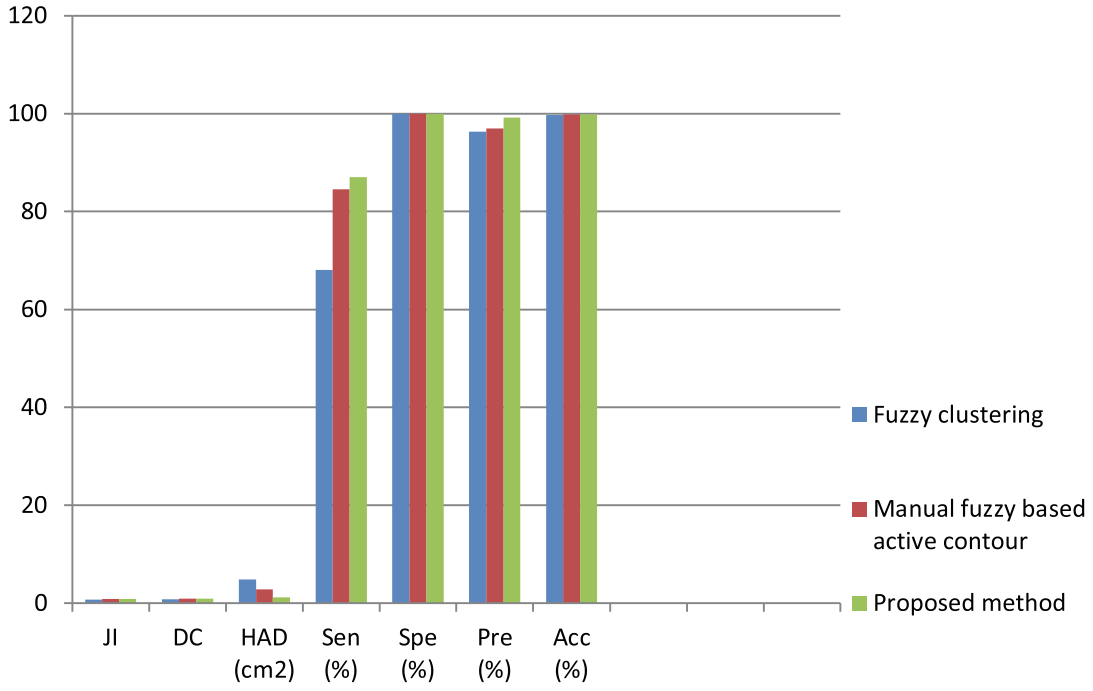

Fig. 8. The summary and comparative analysis of obtained results *Note:* JI: Jacard Index, DC: Dice Coefficient, HAD: Hemorrhage Area Difference, Sen: Sensitivity, SPe: Specificity, Pre: Precision and Acc: Accuracy.

Table 6
Summary of obtained average value for results analysis parameters.

Parameters	Segmentation Method		
	Fuzzy clustering	Manual fuzzy based active contour	Proposed method
Hemorrhagic area difference (cm2)	4.82	2.82	1.21
Sensitivity (%)	68.07	84.55	87.06
Specificity (%)	99.98	99.97	99.98
Precision (%)	96.25	97.02	99.20
Accuracy (%)	99.73	99.83	99.87
Dice coefficient	0.83	0.91	0.930
Jaccard index	0.71	0.84	0.860

The summary and comparative analysis of obtained results are given in Fig. 8.

with average value of 0.71 and 0.84 respectively. Similarly, the values of Dice coefficient are varying from 0.68 to 0.92 for fuzzy clustering method and 0.83–0.96 for manual fuzzy based active contour having average of 0.83 and 0.91 respectively.

The comparative analysis of obtained results in terms of Jaccard index and Dice coefficient for fuzzy clustering method, manual fuzzy based active contour method and proposed method is shown in Fig. 7.

After the comparative analysis of results in terms of Jaccard index and Dice coefficient among fuzzy clustering method, manual fuzzy based active contour method and proposed method found that the maximum Jaccard index is achieved by the proposed segmentation method. The obtained average value of Jaccard index is 0.71 for fuzzy clustering method, 0.84 is for manual fuzzy based active contour method and 0.86 is for proposed method. The obtained average value of Dice coefficient is 0.83 for fuzzy clustering method, 0.91 is for manual fuzzy based active contour method and 0.93 is for proposed method. The obtained value for Jaccard index and Dice coefficient shows that the proposed segmentation method provides better performance and segmented the ICH region more accurately.

4.3. Comparative analysis

The obtained average values for parameters Specificity, Sensitivity, Dice coefficient, Jaccard index, Precision and Accuracy for proposed method for segmentation of ICH regions are summarized in Table 6 and also compared with fuzzy clustering method and manual fuzzy based active contour method for same parameters values for same dataset of testing samples.

From Table 6, it has been observed that proposed method for ICH segmentation using brain CT images yields better performance with respect to fuzzy clustering method and manual fuzzy based active contour method in terms of hemorrhagic area difference, sensitivity, specificity, precision, accuracy, dice index and Jaccard index. Hence the proposed method for ICH segmentation can be recommended as a secondary opinion tool in clinical practice to improve the detection rate.

From Fig. 8 and Table 6, it has been notice that the proposed method for ICH segmentation yields better results in terms of parameters as Jacard Index, Dice Coefficient, Area, sensitivity, specificity, precision and accuracy.

5. Conclusions

Segmentation of ICH hemorrhage is becomes the major task due to high mortality rate. This method improves the accuracy of brain intracranial hemorrhage diagnosis. In this work entropy based automatic unsupervised brain hemorrhage segmentation using fuzzy c-mean with edge-based active contour is used to detect or segment the ICH region on brain CT images. The proposed segmentation technique is the combination of the fuzzy c-mean (FCM) clustering, automatic selection of cluster, skull removal, thresholding and edge-based active contour methods. Experimental Results of ICH segmentation shows that proposed work has highest accuracy than FCM clustering and manual fuzzy based active contour. The proposed automatic segmentation method does not need any experts intervene but manual fuzzy based segmentation method needs of expert. The proposed method can be used for the clinical

Please cite this article as: I. Kumar, C. Bhatt and K. U. Singh, Entropy based automatic unsupervised brain intracranial hemorrhage segmentation using CT images, Journal of King Saud University – Computer and Information Sciences, https://doi.org/10.1016/j.jksuci.2020.01.003

purpose because results of proposed method collaborate well with the experts measurements.

Declaration of Competing Interest

The authors declare that they have no known competing financial interests or personal relationships that could have appeared to influence the work reported in this paper.

References

An, S.J., Kim, T.J., Yoon, B.W., 2017. Epidemiology, risk factors, and clinical features of intracerebral hemorrhage: an update. J. Stroke 19 (1), 3.

Aziz, F., Perwaiz, S., Penupolu, S., Doddi, S., Gongireddy, S., 2011. Intracranial hemorrhage in infective endocarditis: a case report. J. Thoracic Dis. 3 (2), 134.

Bellotti, R., De Carlo, F., Tangaro, S., Gargano, G., Maggipinto, G., Castellano, M., Massafra, R., Cascio, D., Fauci, F., Magro, R., Raso, G., 2006. A completely automated CAD system for mass detection in a large mammographic database. Med. Phys. 33 (8), 3066–3075.

Bezdek, J.C., Pal, S.K., 1992. Fuzzy Models for Pattern Recognition. IEEE Press, New York (Vol. 56).

Bhadauria, H.S., Dewal, M.L., 2014. Intracranial hemorrhage detection using spatial fuzzy c-mean and region-based active contour on brain CT imaging. SIViP 8 (2), 357–364.

Caselles, V., Catté, F., Coll, T., Dibos, F., 1993. A geometric model for active contours in image processing. Numer. Math. 66 (1), 1–31.

Caselles, V., Kimmel, R., Sapiro, G., 1997. Geodesic active contours. Int. J. Comput. Vision 22 (1), 61–79.

Chan, T., 2007. Computer aided detection of small acute intracranial hemorrhage on computer tomography of brain. Comput. Med. Imag. Graph. 31 (4–5), 285–298.

Chan, T., Vese, L., 1999. An active contour model without edges. In: International Conference on Scale-Space Theories in Computer Vision. Springer, Berlin, Heidelberg, pp. 141–151.

Chang, P.D., Kuoy, E., Grinband, J., Weinberg, B.D., Thompson, M., Homo, R., Chen, J., Abcede, H., Shafie, M., Sugrue, L., Filippi, C.G., 2018. Hybrid 3D/2D convolutional neural network for hemorrhage evaluation on head CT. Am. J. Neuroradiol. 39 (9), 1609–1616.

Chen, Y., Chen, G., Wang, Y., Dey, N., Sherratt, R.S., Shi, F., 2019. A Distance Regularized Level-set Evolution Model Based MRI Dataset Segmentation of Brain's Caudate Nucleus. IEEE Access.

Dalyai, M.D., Gonzalez, M.D., Fernando, L., 2011. Case Report on intracranial hemorrhage related to type I cryoglobulinemia. JHN J. 6 (2), 5.

DeLaPaz, R.L., New, P.F., Buonanno, F.S., Kistler, J.P., Oot, R.F., Rosen, B.R., Brady, T.J., 1984. NMR imaging of intracranial hemorrhage. J. Comput. Assist. Tomogr. 8 (4), 599–607.

Dhungel, N., Carneiro, G., Bradley, A.P., 2015, November. Automated mass detection in mammograms using cascaded deep learning and random forests. In: 2015 international conference on digital image computing: techniques and applications (DICTA) (pp. 1–8). IEEE techniques and applications (DICTA) 2015 Nov 23 (pp. 1–8). IEEE.

Feldmann, E., Broderick, J.P., Kernan, W.N., Viscoli, C.M., Brass, L.M., Brott, T., Horwitz, R.I., 2005. Major risk factors for intracerebral hemorrhage in the young are modifiable. Stroke 36 (9), 1881–1885.

Gomez, C.R., 2008. Imaging of Intracranial Hemorrhage. CONTINUUM: Lifelong Learning in Neurology 14.4, pp. 37–56.

Hart, R.G., Lock-Wood, K.I., Hakim, A.M., Koller, R., Davenport, J.G., Coull, B.M., Nath, A., 1984. Immediate anticoagulation of embolic stroke: brain hemorrhage and management options. Stroke 15 (5), 779–789.

Heit, J.J., Michael, L.V., Wintermark, M., 2017. Imaging of intracranial hemorrhage. J. Stroke 19 (1), 11–27.

Hossain, M.S., 2019. Micro calcification segmentation using modified U-net segmentation network from mammogram. J. King Saud Univ.-Comp. Inf. Sci. https://doi.org/10.1016/j.jksuci.2019.10.014.

Howard, G., Cushman, M., Howard, V. J., Kissela, B. M., Kleindorfer, D. O., Moy, C. S., Woo, D. (2013). Risk factors for intracerebral hemorrhage: the REasons for geographic and racial differences in stroke (REGARDS) study. Stroke, STROKEAHA-111.

Kapur, J.N., Sahoo, P.K., Wong, A.K., 1985. A new method for gray-level picture thresholding using the entropy of the histogram. Computer Vision, Graphics, Image Process. 29 (3), 273–285.

Kass, M., Witkin, A., Terzopoulos, D., 1988. Snakes: active contour models. Int. J. Comput. Vision 1 (4), 321–331.

Kooi, T., Litjens, G., Van Ginneken, B., Gubern-Mérida, A., Sánchez, C.I., Mann, R., den Heeten, A., Karssemeijer, N., 2017. Large scale deep learning for computer aided detection of mammographic lesions. Med. Image Anal. 35, 303–312.

Kumar, I., Rawat, J., Bhadauria, H.S., 2014. A conventional study of edge detection technique in digital image processing. Int. J. Comp. Sci. Mobile Comp. 3 (4), 328–334.

Lévy, D. and Jain, A., 2016. Breast mass classification from mammograms using deep convolutional neural networks. arXiv preprint arXiv:1612.00542.

Li, C., Xu, C., Gui, C., & Fox, M. D. (2005, June). Level set evolution without re-initialization: a new variational formulation. In Computer Vision and Pattern Recognition, 2005. CVPR 2005. IEEE Computer Society Conference on (Vol. 1, pp. 430–436). IEEE.

Li, C., Xu, C., Gui, C., Fox, M.D., 2010. Distance regularized level set evolution and its application to image segmentation. IEEE Trans. Image Process. 19 (12), 3243.

Liao, C.C., Xiao, F., Wong, J.M., Chiang, I.J., 2010. Computer-aided diagnosis of intracranial hematoma with brain deformation on computed tomography. Comput. Med. Imaging Graph. 34 (7), 563–571.

Lieberman, A., Hass, W.K., Pinto, Richard, Isom, W.O., Kupersmith, M., Bear, George, Chase, R., 1978. Intracranial hemorrhage and infarction in anticoagulated patients with prosthetic heart valves. Stroke 9 (1), 18–24.

Liscano, R., Wong, A.K.C., 1995. A study into entropy-based thresholding for image edge detection.

Loncaric, S., Dhawan, A. P., Cosic, D., Kovacevic, D., Broderick, J., & Brott, T. (1999, May). Quantitative intracerebral brain hemorrhage analysis. In Medical Imaging 1999: Image Processing (Vol. 3661, pp. 886-895). International Society for Optics and Photonics.

Loncaric, S., Kovacevic, D., & Cosic, D. (1998, May). Fuzzy expert system for edema segmentation. In Electrotechnical Conference, 1998. MELECON 98., 9th Mediterranean (Vol. 2, pp. 1476-1479). IEEE.

Malik, M., Spurek, P., Tabor, J., 2016. Cross-entropy based image thresholding. Schedae Informaticae 24, 21–29.

Mumford, D., Shah, J., 1989. Optimal approximations by piecewise smooth functions and associated variational problems. Commun. Pure Appl. Math. 42 (5), 577–685.

Osher, S., Sethian, J.A., 1988. Fronts propagating with curvature-dependent speed: algorithms based on Hamilton-Jacobi formulations. J. Comput. Phys. 79 (1), 12–49.

Otsu, N., 1979. A threshold selection method from gray-level histograms. IEEE Trans. Syst., Man, Cybernetics 9 (1), 62–66.

Pham, D.L., Prince, J.L., 1999. An adaptive fuzzy segmentation algorithm for three-dimensional magnetic resonance images. In: Biennial International Conference on Information Processing in Medical Imaging. Springer, Berlin, Heidelberg, pp. 140–153.

Pratondo, A., Chui, C.K., Ong, S.H., 2017. Integrating machine learning with region-based active contour models in medical image segmentation. J. Vis. Commun. Image Represent. 43, 1–9.

Punitha, R., Kumar, M.V., Rayamane, A.P., Selvi, L.T., 2014. Natural intracranial hemorrhage and its forensic implications: a case review. J. Indian Acad. Forensic Med. 36 (2), 215–217.

Qaroush, A., Jaber, B., Mohammad, K., Washaha, M., Maali, E., Nayef, N., 2019. An efficient, font independent word and character segmentation algorithm for printed Arabic text. J. King Saud Univ.-Comp. Inf. Sci. https://doi.org/10.1016/j.jksuci.2019.08.013.

Rajinikanth, V., Satapathy, S.C., Fernandes, S.L., Nachiappan, S., 2017. Entropy based segmentation of tumor from brain MR images–a study with teaching learning based optimization. Pattern Recogn. Lett. 94, 87–95.

Rao, R.V., Savsani, V.J., Vakharia, D.P., 2011. Teaching–learning-based optimization: a novel method for constrained mechanical design optimization problems. Comput. Aided Des. 43 (3), 303–315.

Rawat, J., Singh, A., Bhadauria, H.S., Kumar, I., 2014. Comparative analysis of segmentation algorithms for leukocyte extraction in the acute Lymphoblastic Leukemia images. In Parallel, Distributed and Grid Computing (PDGC), 2014 International Conference on (pp. 245-250). IEEE.

Sethian, J.A., 2001. Evolution, implementation, and application of level set and fast marching methods for advancing fronts. J. Comput. Phys. 169 (2), 503–555.

Siddiqui, F.M., Bekker, S.V., Qureshi, A.I., 2011. Neuroimaging of hemorrhage and vascular defects. Neurotherapeutics 8 (1), 28–38.

Tsallis, C., 1988. Possible generalization of Boltzmann-Gibbs statistics. J. Stat. Phys. 52 (1–2), 479–487.

Vakharia, V., Gupta, V.K., Kankar, P.K., 2015. A multiscale permutation entropy based approach to select wavelet for fault diagnosis of ball bearings. J. Vib. Control 21 (16), 3123–3131.

Wang, J., Yang, X., Cai, H., Tan, W., Jin, C., Li, L., 2016. Discrimination of breast cancer with microcalcifications on mammography by deep learning. Sci. Rep. 6, 27327.

Weszka, J.S., Nagel, R.N., Rosenfeld, A., 1974. A threshold selection technique. IEEE Trans. Comput. 100 (12), 1322–1326.

Zaki, W.M.D.W., Fauzi, M.F.A., Besar, R., Ahmad, W.S.H.M.W., 2011. Abnormalities detection in serial computed tomography brain images using multi-level segmentation approach. Multimedia Tools Appl. 54 (2), 321–340.

Zhang, R., Liu, J., 2006. Underwater image segmentation with maximum entropy based on particle swarm optimization (PSO). In: Computer and Computational Sciences, 2006. IMSCCS'06. First International Multi-Symposiums on (Vol. 2, pp. 360-636). IEEE.

Please cite this article as: I. Kumar, C. Bhatt and K. U. Singh, Entropy based automatic unsupervised brain intracranial hemorrhage segmentation using CT images, Journal of King Saud University – Computer and Information Sciences, https://doi.org/10.1016/j.jksuci.2020.01.003